applied sciences

MDPI

Article

Efficient Fractionation of Green Bamboo Using an Integrated Hydrothermal–Deep Eutectic Solvent Pretreatment for Its Valorization

Longjun Chang [1], Ruya Ye [1], Jialing Song [1], Yinuo Xie [1], Qizhen Chen [1], Sien Yan [1], Kang Sun [2,*] and Linhuo Gan [1,*]

[1] College of Chemical Engineering, Huaqiao University, Xiamen 361021, China
[2] Institute of Chemical Industry of Forest Products, Chinese Academy of Forestry, Nanjing 210042, China
* Correspondence: sunkang0226@163.com (K.S.); lhgan401@126.com (L.G.)

Abstract: Adopting an integrated strategy to realize efficient fractionation of lignocellulose into well-defined components for its valorization is challenging. Combinatorial pretreatments in this study decomposed hemicellulose of green bamboo during hydrothermal pretreatment (HP), and the hydrothermally pretreated bamboo was subsequently subjected to delignification using deep eutectic solvent (DES) consisting of choline chloride and lactic acid, finally facilitating enzymatic hydrolysis of cellulose residue. Upon hydrothermal treatment at 180 °C for 35 min, hemicellulose removal of 88.6% was achieved with xylo-oligosaccharide yield and purity of 50.9% and 81.6%, respectively. After DES treatment at 140 °C for 2 h, lignin removal was determined to be 79.1%. Notably, the regenerated lignin with high purity of 96.8% displayed superior antioxidant activity, and the decrease in the ratio of syringyl units to guaiacyl units led to a slight decrease in radical scavenging activity of lignin after five recycling runs of DES. Moreover, the two-step treated residue had much higher enzymatic digestibility than that of single HP residue and untreated green bamboo. Results show that synergistic pretreatment is a promising strategy to tackle the recalcitrance of lignocellulose towards high value-added utilization.

Keywords: bamboo; hydrothermal; deep eutectic solvent; enzymatic hydrolysis; antioxidant

check for updates

Citation: Chang, L.; Ye, R.; Song, J.; Xie, Y.; Chen, Q.; Yan, S.; Sun, K.; Gan, L. Efficient Fractionation of Green Bamboo Using an Integrated Hydrothermal–Deep Eutectic Solvent Pretreatment for Its Valorization. *Appl. Sci.* **2023**, *13*, 2429. https://doi.org/10.3390/app13042429

Academic Editor: Antonio Valero

Received: 27 January 2023
Revised: 11 February 2023
Accepted: 11 February 2023
Published: 14 February 2023

Copyright: © 2023 by the authors. Licensee MDPI, Basel, Switzerland. This article is an open access article distributed under the terms and conditions of the Creative Commons Attribution (CC BY) license (https://creativecommons.org/licenses/by/4.0/).

1. Introduction

China, as one of the world's largest carbon emitters, has proposed the goal of carbon neutrality by 2060 [1]. The development of clean and renewable energy sources, such as wind power, solar power, hydropower, nuclear power, and biomass power, is an efficient solution to achieve this challenging goal [2,3]. Among them, biomass, especially lignocellulose, is an abundant, readily available, and sustainable resource. As is known, bamboo is a typical kind of lignocellulosic biomass with approximately 1500 species under 87 genera, and the total forest area of bamboo in China is approximately 6 million hectares [4,5]. Notably, bamboo grows rapidly (a peak growth rate up to 100 cm per day) and can be harvested every 3–5 years, well exceeding the growth rate (typically 0.1–0.4 cm per day) and the 20–60-year growth cycle of traditional timber [6]. Consequently, bamboo is widely treated as a substitute for woody biomass, exerting enormous influence in easing the pressure on traditional timber [7].

However, the high-value utilization of lignocellulose is generally hampered by its structural recalcitrance to a large extent. It is commonly believed that the recalcitrant and rigid characteristics of lignocellulose are derived from its integral compact structure. To disrupt the compact structure of lignocellulose, tremendous pretreatment techniques have been developed [8–11]. Compared with other pretreatment techniques, hydrothermal pretreatment has various advantages such as high separation efficiency, high throughput, and the possibility of coordination with other pretreatment techniques [12]. During

hydrothermal pretreatment, hydronium ions, generated from water auto-ionization, and carboxylic acids, liberated from deacetylation of hemicellulose, act as hydrolytic catalysts [13,14]. Rather than cellulose, hemicellulose is much less resistant to hydrolysis [15]. Zheng et al. [16] showed that 80.2% of bamboo hemicellulose was dissolved during hydrothermal pretreatment at 180 °C for 90 min. Xiao et al. [17] studied the hydrothermal pretreatment of bamboo for xylo-oligosaccharide production, and their maximum recovery yield of xylo-oligosaccharides was 47.5% at 180 °C for 30 min. Huang et al. [18] demonstrated that the highest xylo-oligosaccharide concentration of 10.5 g/L was obtained during hydrothermal pretreatment of bamboo at 180 °C for 40 min. However, due to the unintended hydrolysis of xylo-oligosaccharides, the yield of xylo-oligosaccharides from bamboo was only around 8.0% via hydrothermal pretreatment at 200 °C for 60 min [19].

It is generally acknowledged that lignin cannot be easily deconstructed using hydrothermal pretreatment [18], whereas deep eutectic solvent (DES) can easily dissolve lignin [20,21]. DES also has promising properties such as non-toxicity, low volatility and flammability, biocompatibility, low cost, and ease of synthesis [22–24]. Fernandes et al. [25] revealed that choline chloride (ChCl)-based DES was more efficient in delignification than betaine- or urea-based DES. Komesu et al. [26] pointed out that lactic acid (LA) could be manufactured via fermentation from agricultural products and exhibited high thermal stability with an evaporation temperature of ∼180 °C. Tan et al. [27] investigated the effect of functional groups in carboxylic acid on lignin extraction, demonstrating that a short alkyl chain and an extra α-hydroxyl group enhanced the extraction rate of lignin. Therefore, ChCl–LA DES is widely used in the delignification of lignocellulose [28–30]. For example, Wang et al. [28] demonstrated that the delignification of bamboo using ChCl–LA DES (80.1%) was much higher than that using betaine–LA DES (54.5%) at 140 °C for 6 h. Although ChCl–LA DES exhibits a superior performance in delignification as well as hemicellulose removal, hemicellulose was usually treated as waste in DES liquid [29,30].

The total content of hemicellulose, cellulose, and lignin in bamboo is between 89 and 93% [5]. It is known that hemicellulose and cellulose can be used for the production of bio-ethanol as well as platform chemical production, and lignin, the most abundant natural source of aromatic compounds, can also be regarded as a promising alternative to fossil-based resources in energy and chemical industries. Therefore, pursuing fractionation of lignocellulose into three main separated components, and further realizing its comprehensive and value-added utilization is of great significance. Additionally, Questell-Santiago et al. [14] pointed out that biomass-deconstruction treatment starting with hemicellulose and lignin decomposition before cellulose depolymerization tended to be kinetically more favorable, and developing an integrated approach to achieve efficient fractionation of lignocellulose was always challenging. Hence, this work aimed to systematically study the fractionation of green bamboo via an integrated hydrothermal–DES pretreatment, where hydrothermal treatment selectively degraded hemicellulose into xylo-oligosaccharides and swelled up the cell wall structures of bamboo, contributing to the sequential delignification via ChCl–LA, and finally facilitating the enzymatic hydrolysis of crude cellulose. In brief, this study hopes to shed light on the biorefinery through investigating the effects of the integrated hydrothermal–DES pretreatment on enzymatic digestibility of green bamboo. In this study, hydrothermal and DES treatment processes were thoroughly optimized; the crystallinity and structural properties of bamboo residue after hydrothermal and DES treatments were also comparatively investigated using an X-ray diffractometer (XRD), Fourier-transform infrared (FTIR) spectroscopy, and field-emission scanning electron microscopy (FE–SEM). In addition, heteronuclear single quantum correlation nuclear magnetic resonance (HSQC–NMR) was employed to characterize the structure of DES-extracted lignin (DEL), and the antioxidant activity of DEL was also evaluated.

2. Materials and Methods

2.1. Materials

Green bamboo (*Dendrocalamopsis oldhami*) culms and long-staple cotton were kindly provided by local processing factories (Fujian, China), 40–60 mesh ground bamboo fractions were employed as experimental feedstock. The principal component analysis of bamboo followed the sequential gravimetric method [31,32] with hemicellulose, lignin, and cellulose, respectively accounting for 20.7%, 24.8%, and 52.2%. ChCl (AR, 98%), D-(+)-Xylose (≥99%), and 1,1-diphenyl-2-picrylhydrazyl (DPPH) were purchased from Shanghai Aladdin Biochemical Technology Co., Ltd. (Shanghai, China). LA (AR, 85.9–90.0%) and D-Glucose (AR) were purchased from Xilong Scientific Co., Ltd. (Shantou, China). Cellulase (Cellic CTec3) was provided by Novozymes (Beijing, China) with a measured filter paper activity of 260.0 FPU/mL. Cellulase (PH9018, 1/3 of the price of Cellic CTec3) with a measured filter paper activity of 200.0 FPU/g, Tween-20, and bovine serum albumin (BSA) were generously provided by Phygene Biotechnology Co., Ltd. (Fuzhou, China). All other reagents were of analytical grade and used as received.

2.2. DES Preparation

ChCl–LA (1:3 to 1:15) was prepared by mixing ChCl with LA and stirring at 60 °C until a homogeneous and transparent solution was obtained.

2.3. Hydrothermal Treatment

The combinatorial pretreatments for bamboo fractionation were sequentially performed with hydrothermal and DES treatments, as shown in Figure 1. During hydrothermal treatment, the experiments were conducted in a batch reactor (SLM 250, Beijing Century Senlong experimental apparatus Co., Ltd., Beijing, China). Specifically, 3.0 g dry bamboo powder was mixed with a certain amount of distilled water depending on the specified solid-to-liquid ratio. Hydrothermal parameters including temperature (160–210 °C), time (20–50 min), and solid-to-liquid ratio (1:8–18, w/v) were investigated using a single-factor experimental method. The agitation rate of magnetic stirring was set at 350 rpm. The air that remained in the reactor was driven out using nitrogen purging. The mixture was then heated up to a target temperature for a designed period of time. Upon completion of the reaction, the reactor was immediately quenched in an ice–water bath to stop the reaction. The mixture was separated using low-pressure filtration; the filtrate was collected and concentrated using rotary evaporation at 65 °C. Anhydrous ethanol was then used as an antisolvent to precipitate xylo-oligosaccharides at a volume ratio of 5:1. The subsequent centrifugation and freeze-drying procedures were performed to obtain xylo-oligosaccharides. The hydrothermally treated bamboo (HTB) was then washed with distilled water until the effluent turned colorless and oven-dried at 105 °C to a constant weight.

Additionally, the severity factor (log R_0, as shown in Equation (1)) was employed to consider the combined effects of hydrothermal temperature and time. Both heating and cooling stages were taken into account to reduce the error [33]:

$$\log R_0 = \log \left(\int_0^t \exp\left[\frac{T(t)-100}{14.75}\right] \mathrm{d}t \right), \quad (1)$$

where t (min) is the reaction time, and $T(t)$ (°C) is the experimental temperature for t. The records of experimental temperatures to reaction times under different hydrothermal conditions can be referred to in Figure S1.

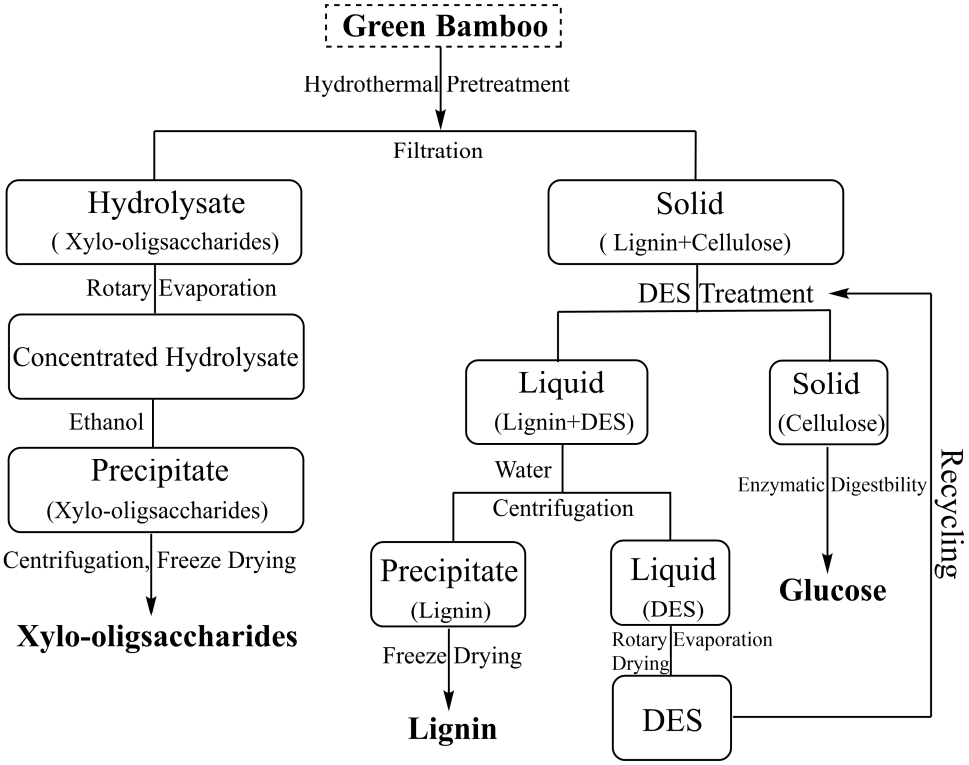


Figure 1. Flowchart of the fractionation of green bamboo using sequential hydrothermal and DES treatments.

2.4. DES Treatment

Sequentially, HTB obtained under the optimal hydrothermal parameters was subjected to ChCl–LA treatment for further delignification. A single-factor experimental method was also employed to optimize the parameters in DES treatment, including molar ratio of ChCl to LA (1:3–15), temperature (90–160 °C), time (1–5 h), solid-to-liquid ratio (1:10–30, w/v), and water content (0–60%, v/v). In detail, 1.0 g HTB was mixed with a defined amount of DES and incubated at a target temperature with magnetic agitation for a certain period. After the reaction, the reaction apparatus was cooled down at RT. The cellulose-rich residue (CR) was separated using vacuum filtration and the filtrate was collected. Distilled water was then introduced at a volume ratio of water/filtrate of 9:1 to drive lignin precipitation. Lignin precipitates were obtained using centrifugation at 10,000 rpm for 5 min and washed with additional ethanol/water (1:9, v/v) solution. Finally, DEL was obtained using freeze-drying. CR was then washed with an excessive amount of water and oven-dried at 105 °C to a constant weight.

To recycle DES, the effluents were collected and concentrated at 65 °C using rotary evaporation, and then oven-dried at 105 °C to obtain anhydrous DES.

2.5. Analysis of Antioxidant Activity of Regenerated Lignin

The antioxidant activity of DEL was evaluated based on its radical scavenging properties following a previously reported method [34]. Lignin samples were dissolved in dioxane/water solution (9:1, v/v), and aqueous dioxane solutions (3.8 mL) with different concentrations (0.05, 0.1, and 0.2 mg/mL) were mixed with 11.8 mL of a 6.1 $\times$ 10^{-5} mol/L DPPH methanol solution at 25 °C for 16 min. The concentrations of DPPH radicals at 0 and 16 min were measured at 516 nm (λ_{max}) using a UV-vis spectrometer. The inhibitory ratio (IP) of the DPPH radials was calculated using Equation (2).

$$IP = \frac{A_2 - A_1 + A_0}{A_2} \times 100\%, \quad (2)$$

where A_2 is the absorbance at 0 min; A_1 is the absorbance at 16 or 60 min; and A_0 is the absorbance of the blank solution.

2.6. Enzymatic Hydrolysis of Green Bamboo Cellulose

CR pretreated under the optimal hydrothermal–DES parameters was exploited to perform enzymatic hydrolysis in 0.05 M sodium citrate buffer (pH 4.8) at 50 °C and 150 rpm for 72 h. Upon completion of enzymatic hydrolysis, the supernatant was boiled for ~10 min to stop the hydrolysis reaction, filtered using syringe filters (0.22 μm), and then analyzed via high-performance liquid chromatography (HPLC) for glucose content. Enzymatic parameters including solid loading (2–10%, w/v), chemical additive (Tween-20, BSA, 5–25 mg/mL), cellulase dosage (30–90 FPU/g_{glucan}), and the composition of cellulase complexes (Cellic CTec3, PH9018, 0–100%) were thoroughly investigated using a single-factor experimental method. The saccharification ratio was defined as described in Equation (3).

$$Saccharification\ Ratio\ (\%) = \frac{Amount\ of\ glucose\ produced\ (g)}{Amount\ of\ cellulose\ in\ the\ solid\ residue\ (g)\ \times\ 1.11} \times 100\% \quad (3)$$

2.7. Determination of Lignin Purity

Lignin purity was determined according to NREL procedures [35]. Briefly, 0.3 g lignin sample was subjected to hydrolysis with 3.0 mL sulfuric acid (72% H_2SO_4) at 30 °C for 60 min. Upon completion of the sulfuric acid hydrolysis, 84.0 mL deionized water was supplemented to dilute the acid to a 4% concentration. The mixture was incubated at 121 °C for 60 min. The acid-insoluble fraction was separated using low-pressure filtration and oven-dried at 105 °C. The amount of acid-insoluble ash was measured at 575 °C. The acid-soluble lignin was measured at a wavelength of 205 nm. Results showed that 85.2% of bamboo lignin with a purity of 96.8% was recovered.

2.8. Analytical Methods

The analysis of the hydrothermal hydrolysate was conducted using HPLC (Agilent 1260 II, Germany). Firstly, the hydrolysate was subjected to hydrolysis with dilute sulfuric acid (4% H_2SO_4) at 121 °C for 60 min to convert xylo-oligosaccharides to xylose, and the quantity of xylo-oligosaccharides was expressed as monosaccharides equivalents [17]. The post-hydrolysate was then filtered through syringe filters (0.22 μm) and analyzed using HPLC with a refractive index detector using a ZORBAX carbohydrate analysis column at 25 °C. A volume of 15 μL filtrate was injected by an autosampler and the mobile phase was a mixture of acetonitrile and water (90:10, v/v), with a flow rate of 1.1 mL/min. The deashing guard column was placed ahead of the analysis column. It should be noted that these procedures were also employed to determine the purity of as-obtained xylo-oligosaccharides. The yield of xylo-oligosaccharides from bamboo hemicellulose was determined to be 50.9% with a purity of 81.6%. In addition, the quantitative analysis of glucose content during enzymatic saccharification was also analyzed using HPLC with a refractive index detector using a ZORBAX carbohydrate analysis column at 30 °C. A volume of 20 μL filtrate was injected by an autosampler and the mobile phase was a mixture of acetonitrile and water (75:25, v/v), with a flow rate of 1.0 mL/min.

The surface morphology of samples was observed using FE–SEM (S-4800, Hitachi, Tokyo, Japan). The samples were coated with gold and photographed at 5.0 kV, 10 μA.

The measurement of FTIR spectroscopy was performed on an FTIR spectrophotometer (Nicolet iS50, ThermoFisher, MA, USA) with a scanning range of 4000–400 cm^{-1} and an accumulation of 32 scans.

X-ray diffraction was conducted on an X-ray powder diffractometer (X'Pert Pro, Panalytical, Almelo, Holland) with Cu-Kα radiation. The spectra were collected at 2θ of 5–60° with a scan speed of 0.2°/s and a step size of 0.02°. The acceleration voltage and

current were 40 kV and 40 mA, respectively. The crystallinity index (*CrI*) was determined according to Equation (4) reported by Segal et al. [36]:

$$CrI = \frac{I_{002} - I_{am}}{I_{002}} \times 100\%, \quad (4)$$

where *CrI* represents the relative degree of crystallinity, I_{002} is the intensity of (002) lattice diffraction at 2θ = 22.8°, and I_{am} is the diffraction intensity of amorphous scattering at 2θ = 18.0°.

The specific surface area of untreated bamboo, HTB, and CR were determined using N_2 adsorption/desorption isotherms using the Brunauer–Emmett–Teller (BET) equation on an automated physisorption analyzer (3Flex, Micromeritics, GA, USA) at 77 K. Results showed that there was no significant difference among untreated bamboo, HTB, and CR with respect to BET surface area (around 1.0 m^2/g).

HSQC–NMR spectra were recorded on a Bruker AVANCE III 500 MHz NMR spectrometer (Bruker, Zurich, Switzerland). For HSQC spectroscopy, around 80 mg of lignin was dissolved in 0.5 mL deuterated dimethylsulfoxide (DMSO-d_6). The spectral widths were 12–0 and 160–0 ppm for ^1H and ^{13}C dimensions, respectively. The chemical shift of DMSO-d_6 at δ_C/δ_H 39.5/2.49 ppm was treated as an internal reference. Data of spectra were processed using Bruker Topspin 3.6.2 (Bruker, Karlsruhe, Germany)

3. Results

3.1. Hydrothermal Treatment

3.1.1. Hydrothermal Parameter Optimization

Figure 2a shows the impact of hydrothermal temperature on xylose concentration. An initial increase in xylose concentration with increasing temperature (160–180 °C) indicates that more hemicellulose was decomposed compared to the corresponding xylo-oligosaccharides with an increase in log R_0 from 3.4 to 3.9 and a pH drop from 4.6 to 3.9 (Figure 2g). In addition, a dramatic decline was observed as hydrothermal temperature exceeded 190 °C, which is probably due to the formation of furfural [37]. The concentration of xylose reached its maximum value of 9.4 mg/mL at 180 °C. Meanwhile, the hemicellulose removal was 80.4%, and the retention of cellulose and lignin was 97.8% and 82.5%, respectively, as exhibited in Figure 2d. The effects of hydrothermal time and solid-to-liquid ratio were also investigated, as shown in Figure 2b,c,e,f. The maximum xylose concentration of 10.5 mg/mL was obtained under the optimal conditions of 180 °C, 35 min, and 3:30 g/mL. Meanwhile, the hemicellulose removal is 88.6%, and the retention of cellulose and lignin was 96.3% and 79.1%, respectively.

Furthermore, as shown in Figure 2g–i, hydrothermal temperature exerts an influence on green bamboo deconstruction with the most significant pH drop from 4.6 to 3.4, probably due to water auto-ionization and carboxylic acids liberated during the deacetylation of hemicellulose [13,14].

3.1.2. Micromorphology Analysis of HTB

Figure S2 shows the surface morphology of untreated bamboo and HTB prepared under different hydrothermal conditions. When the hydrothermal temperature exceeds the phase transition temperature of lignin, molten lignin tends to coalesce and migrate from the cell walls of a plant, then redeposit on the surfaces of cell walls in the morphology of flattened disks or spherical droplets during cooling [38]. In this study, small lignin droplets (~2 μm) migrated from the cell wall of bamboo and redeposited on its surface as hydrothermal temperature reached 200 °C, as shown in Figure 3b. The morphology of HTB obtained under the optimal hydrothermal conditions is shown in Figure S2i. Compared with the compact, smooth, and rigid morphology of untreated bamboo (Figure S2a), it is believed that the loosened and coarse microstructure of HTB is more beneficial to the sequential DES delignification.

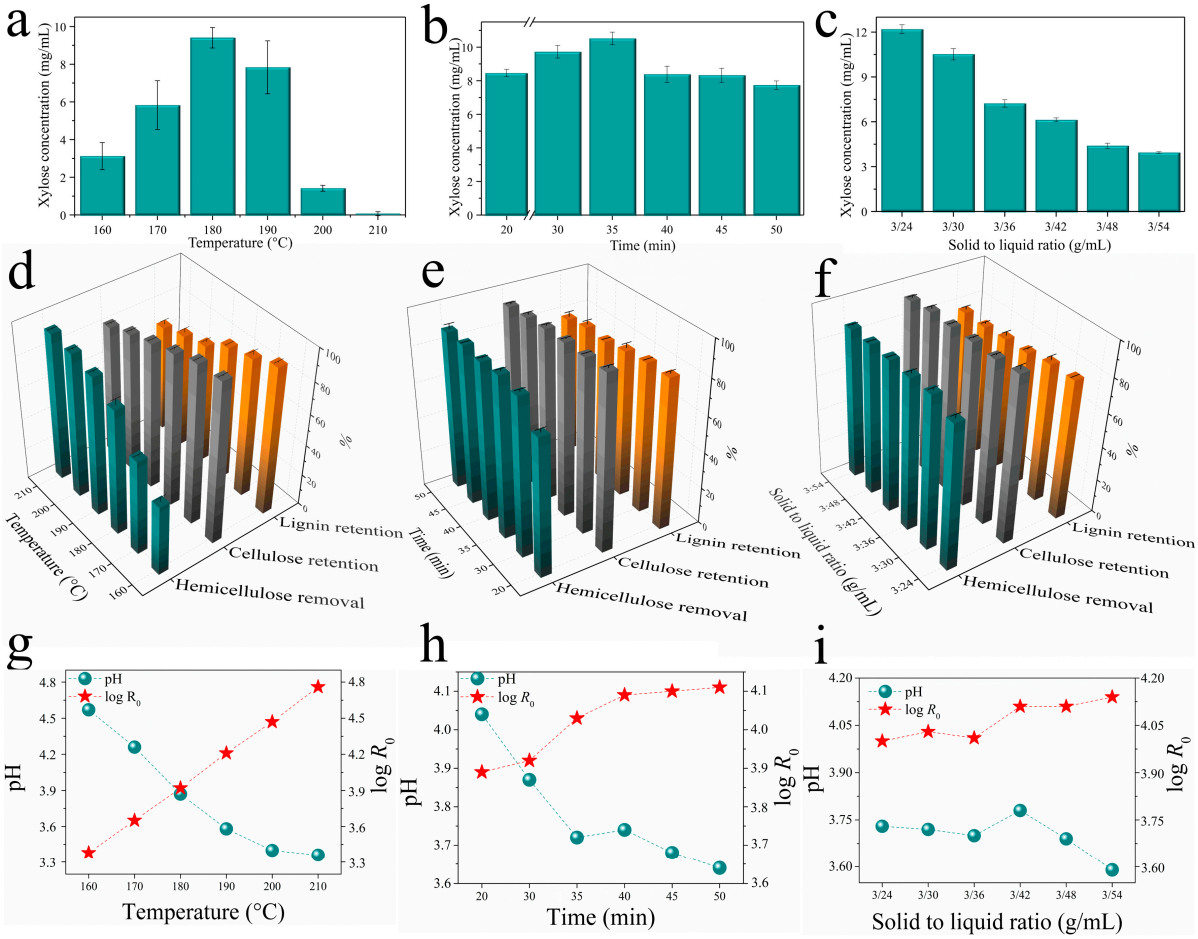


Figure 2. Effects of hydrothermal treatment (**a**) temperature, (**b**) time, and (**c**) solid-to-liquid ratio on xylose concentration in hydrolysate; effects of hydrothermal treatment (**d**) temperature, (**e**) time, and (**f**) solid-to-liquid ratio on the removal of hemicellulose and the retention of cellulose and lignin in HTB; effects of hydrothermal treatment (**g**) temperature, (**h**) time, and (**i**) solid-to-liquid ratio on hydrothermal severity and pH of hydrolysate.

3.1.3. FTIR and XRD Analysis of HTB

FTIR and XRD analyses of HTB prepared under different temperatures were thoroughly investigated, as shown in Figure 3. The FTIR signal assignments are ascribed according to published papers [39–47], as listed in Table S1. The intensified FTIR signals at 1514 (aromatic skeletal vibrations in lignin), and 1060 and 1030 cm^{-1} (characteristic stretching in cellulose) after hydrothermal treatment (Figure 3a) elucidate that the substantial removal of hemicellulose facilitates the exposure of cellulose and lignin, which was demonstrated by lignin droplets in Figure 3b.

XRD was employed to estimate crystallinity of HTB prepared under different hydrothermal temperatures. The characteristic diffraction peaks at 16.4°, 22.5°, and 34.5°, corresponding to (101), (002), and (004) lattice planes, exhibit a typical cellulose I crystalline structure [48]. *CrI* is related to the stiffness and strength of fibers; a higher *CrI* implies a more crystalline and ordered structure [48]. As seen from the inset plots in Figure 3c, *CrI* was gradually enhanced with the increase in hydrothermal temperature, highlighting that hydrothermal treatment is an efficient way to remove amorphous portions of bamboo, and *CrI* increased dramatically when the temperature exceeded 190 °C, which is probably related to the further removal of amorphous lignin, as illustrated in Figure 2d.

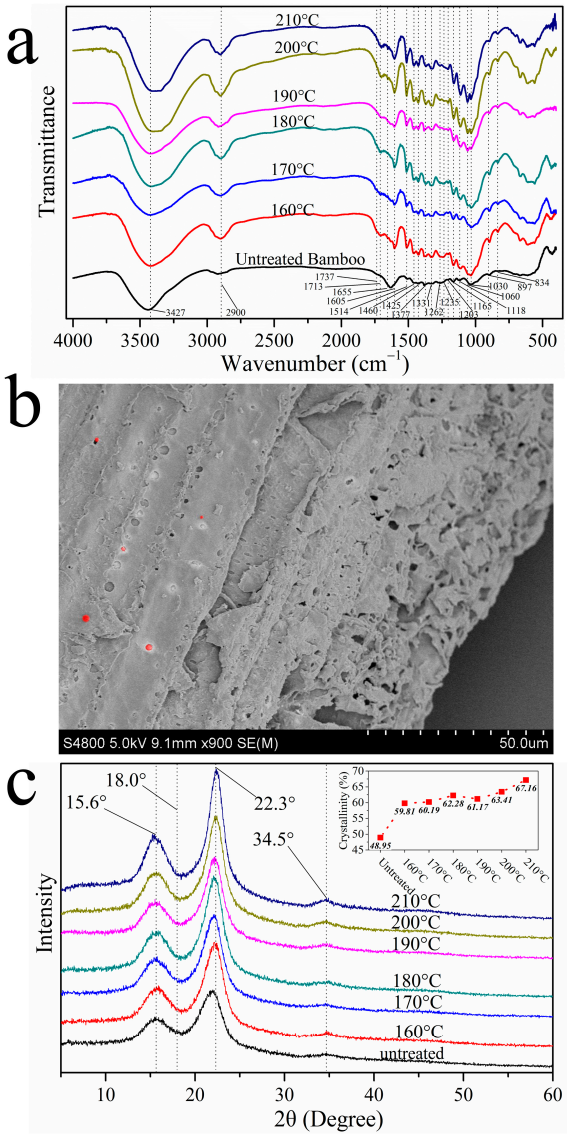


Figure 3. (**a**) FTIR spectra of HTBs prepared under different hydrothermal temperatures, (**b**) lignin droplets on HTB obtained under hydrothermal conditions of 200 °C, 30 min, 3/30 g/mL, (**c**) XRD spectra and *CrI* of HTB prepared under different hydrothermal temperatures.

3.2. DES Treatment

3.2.1. Optimization of the DES Treatment Process

It was found that the treatment temperature and additional water supplementation exert pronounced influence on lignin removal, as shown in Figure 4 (II) and (V), while the effects of molar ratio of ChCl to LA, treatment time, and solid-to-liquid ratio of HTB to DES on delignification were not obvious. Specifically, there was a dramatic increase in lignin removal with increasing temperature from 110 °C to 140 °C. It is proposed that a high temperature results in a decrease in viscosity and surface tension, leading to an enhancement in diffusivity of mass transfer [49]. In addition, it is known that water frequently serves as a supplementary component in DES systems to lower the viscosity and density of the mixture [50]. However, it is observed from Figure 4 (V) that delignification efficiency decreases significantly with additional water supplementation. Therefore, anhydrous ChCl–LA is more beneficial to delignification. To conclude, the lignin removal and cellulose retention were 79.1% and 81.7%, respectively, under the optimal conditions of 1:3 of ChCl:LA, 140 °C, 2 h, and 1/10 (w/v) of solid-to-liquid ratio of HTB to DES.

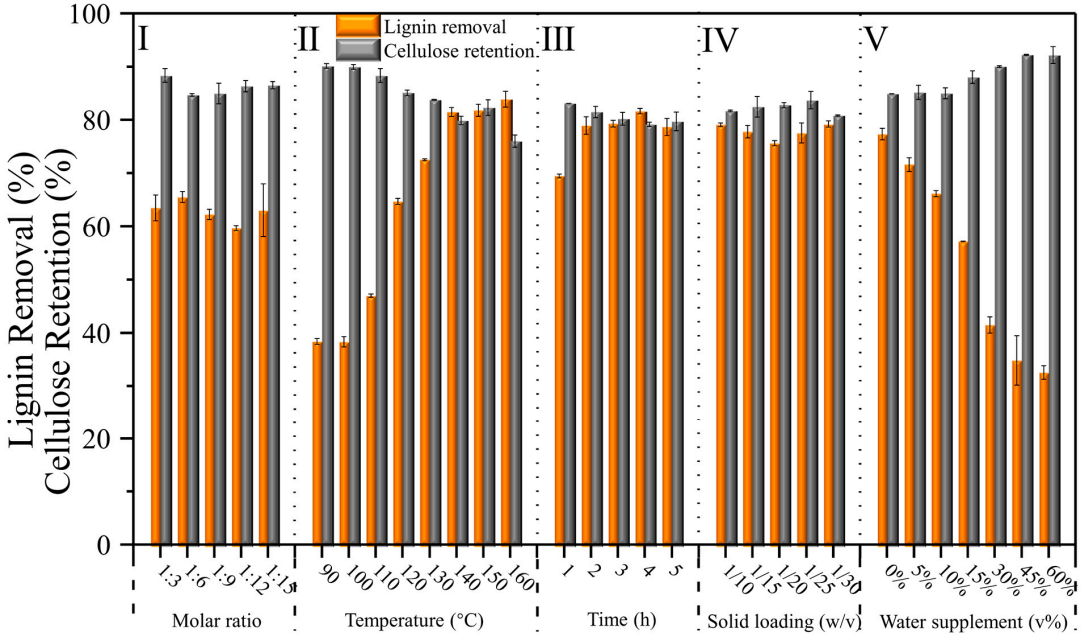


Figure 4. Lignin removal and cellulose retention under DES treatment conditions of: (**I**) molar ratio of ChCl to LA of 1:3–1:15, 120 °C, 3 h, 1:25 g/mL without water addition; (**II**) molar ratio of ChCl to LA of 1:3, 90–160 °C, 3 h, 1:25 g/mL without water addition; (**III**) molar ratio of ChCl to LA of 1:3, 140 °C, 1–5 h, 1:25 g/mL without water addition; (**IV**) molar ratio of ChCl to LA of 1:3, 140 °C, 2 h, 1:10–1:30 g/mL without water addition; (**V**) molar ratio of ChCl to LA of 1:3, 140 °C, 2 h, 1:10 g/mL, and water addition of 0–60% (v%).

3.2.2. FTIR and XRD Analysis of CR

It is concluded from Section 3.2.1 that temperature and additional water supplementation are crucial factors during DES treatment; FTIR and XRD analyses of CR prepared under different treatment temperatures and water addition were therefore thoroughly investigated, as shown in Figure 5a–d. The signal at 1737 cm^{-1} in Figure 5a is strengthened significantly and enhanced with the increase in treatment temperature. In general, the signal at 1737 cm^{-1} is deemed the carbonyl stretching of acetyl or carboxylic groups [41]. It is known that pseudo-lignin containing carbonyl, carboxylic, aliphatic, and aromatic structures can be derived from the degradation of cellulose, especially in the company of high temperatures, acids, and oxygen [51–53]. Thus, α-cellulose and long-staple cotton were selected to be treated with ChCl–LA (Figure 5e), and the presence of an obvious and strong signal at 1737 cm^{-1} in the FT-IR spectra of (ChCl–LA)-treated α-cellulose and (ChCl–LA)-treated cotton probably verify the transformation of cellulose to pseudo-lignin [51]. The other possible reason for the newly generated signal at 1737 cm^{-1} is the esterification of LA with hydroxyl groups of cellulose [54]. In Figure 5b, the signal at 1514 cm^{-1} becomes stronger as the water content increases from 0% to 60%, reflecting that water addition in ChCl–LA exerts a negative effect on delignification, which further demonstrates the conclusion drawn in Section 3.2.1 that anhydrous ChCl–LA is more beneficial to delignification.

Seen from Figure 5c, the *CrI* of HTB was 60.3%, and an initial increase in *CrI* of CR may suggest effective removal of the amorphous portion (mainly lignin) and an enhanced exposure of crystalline cellulose [22], while a gradual decrease in *CrI* could be seen when the temperature was increased from 110 °C to 160 °C, probably indicating that the ordered polymer chain of bamboo cellulose was disrupted. However, it is observed in Figure 5d that the *CrI* of CR increased first and then nearly reached a plateau when the water content in ChCl–LA was higher than 10%. It is suggested that excessive water addition to ChCl–LA leads to a limited disruption to lignocellulosic structure. In addition, XRD spectra of α-cellulose and long-staple cotton before and after ChCl–LA treatment are exhibited in

Figure 5f, and the results verify that ChCl–LA treatment can increase the *CrI* of cellulose or cellulose-rich biomass.

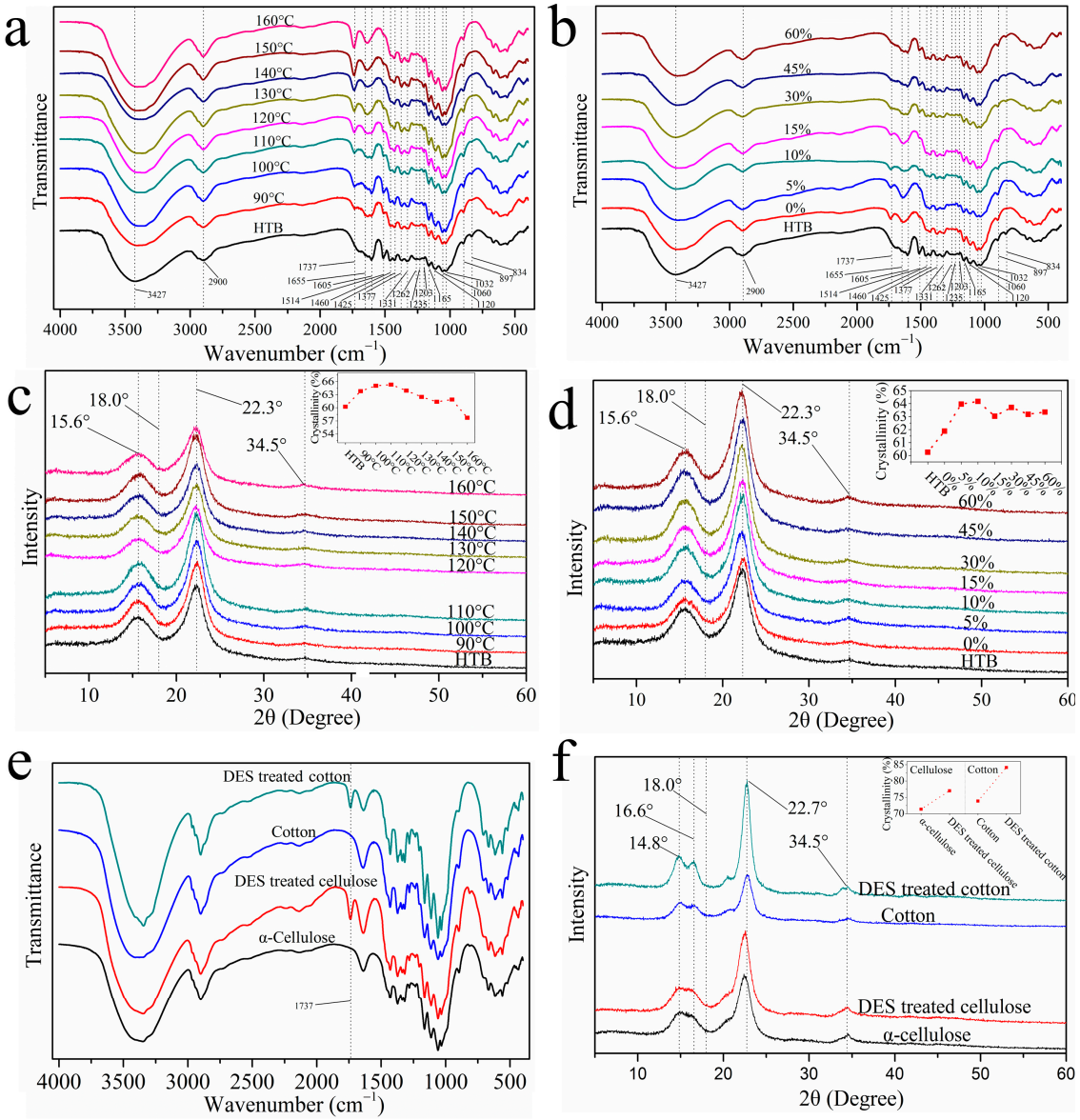


Figure 5. FTIR analysis of CR prepared under (**a**) ChCl:LA (1:3), 90–160 °C, 3 h, 1:25 g/mL without water addition, (**b**) ChCl:LA (1:3), 140 °C, 2 h, 1:10 g/mL, and water addition of 0–60% (v%); XRD analysis of CR prepared under (**c**) ChCl:LA (1:3), 90–160 °C, 3 h, 1:25 g/mL without water addition, (**d**) ChCl:LA (1:3), 140 °C, 2 h, 1:10 g/mL, and water addition of 0–60% (v%); (**e**) FTIR and (**f**) XRD analysis of *α*-cellulose and cotton before and after DES treatment.

3.2.3. DES Recycling Assessment

The recycling of DES is crucial in the reduction in operating cost and meets the requirements of green chemistry. Herein, recycling experiments were carried out under the optimal DES treatment conditions mentioned above. Figure 6a shows the recycling performance of ChCl–LA on the fractionation of green bamboo. Contrary to CR yield and cellulose retention, lignin removal exhibited a decreasing trend with increasing run number, which is probably related to the decrease in acidity and the increase in viscosity and impurity of recycled DES [55–57]. Although it requires in-depth understanding of the recycling performance of recycled DES, the recycling assessment clearly demonstrates that

ChCl–LA can be recycled and reused, exhibiting the potential to reduce the operating cost for industrial consideration.

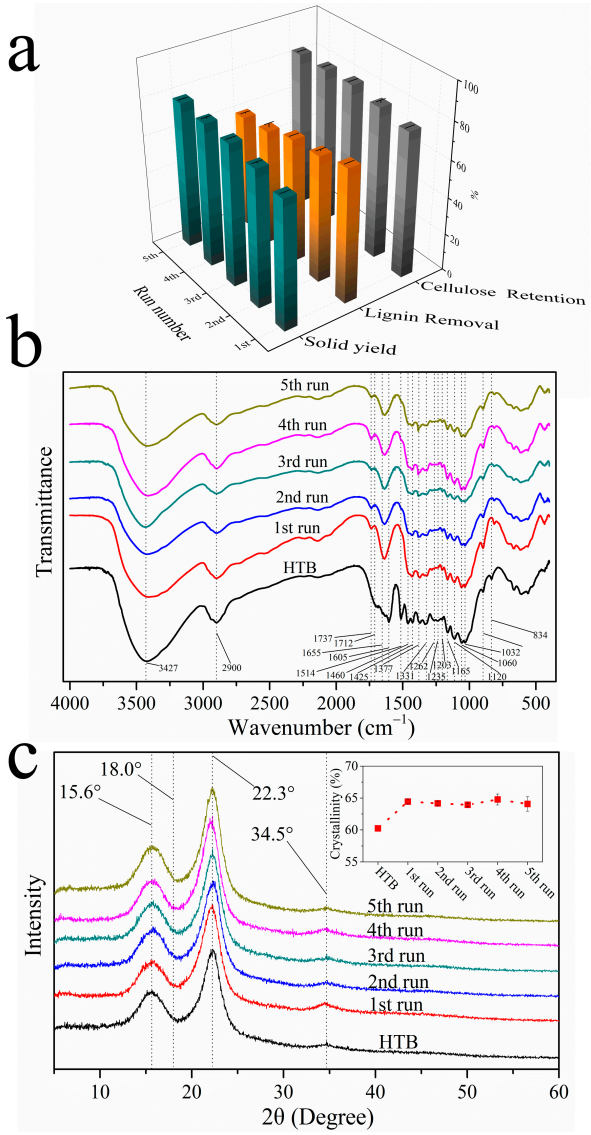


Figure 6. (**a**) Investigation of DES recycling on solid yield, lignin removal, and cellulose retention, (**b**) FTIR spectra of HTB and CR treated with recovered DES, (**c**) XRD spectra of HTB and CR treated with recovered DES.

The weak FTIR signals corresponding to lignin (Figure 6b) and the similar *CrI* of CR (Figure 6c) indicate that ChCl–LA can be recycled five times without a significant decrease in delignification efficiency. Additionally, Wang et al. [58] pointed out that when the residual lignin was less than 36.0%, the adverse effect of lignin on enzymatic hydrolysis efficiency via non-productive enzyme adsorption and steric hindrance was not remarkable. Therefore, achieving complete removal of lignin from bamboo may not be essential and cost-effective for the following saccharification process of CR.

It is generally believed that HSQC–NMR is a powerful technique for lignin structural characterization. The side-chain (δ_C/δ_H 50–95/2.5–6.0 ppm) and aromatic (δ_C/δ_H 95–160/5.5–8.5 ppm) regions of HSQC spectra of DEL after the 1st and 5th run of DES recycling are presented in Figure 7. The main cross-signals are assigned according to previous publications [47,59–63], as listed in Table S2. A correlation for the γ-position cross-signal of the β-O-4′ (A) substructure is observed at δ_C/δ_H 59.8/3.73 ppm, while a

C_γ–H_γ correlation of γ-acylated A can be seen at δ_C/δ_H 63.0/4.30 ppm, and acylation probably occurs between the hydroxyl group at the γ-position of lignin and the carboxyl group in lactic acid [62]. It is believed that ferulate (FA) is responsible for cross-linking in the cell wall of grasses [59], and a C_2–H_2 correlation of FA can be observed at δ_C/δ_H 110.2/7.30 ppm, implying that a slight amount of FA is still associated with lignin [64]. Furthermore, the contents of guaiacyl- (G), syringyl- (S), and *p*-hydroxyphenyl (H)-type lignin substructures, as well as the S/G ratio are inset in Figure 7. Since the value of S/G decreases dramatically from 11.6 to 3.4, S-type lignin substructures were probably demoxylized and partially converted to G-type lignin substructures [16].

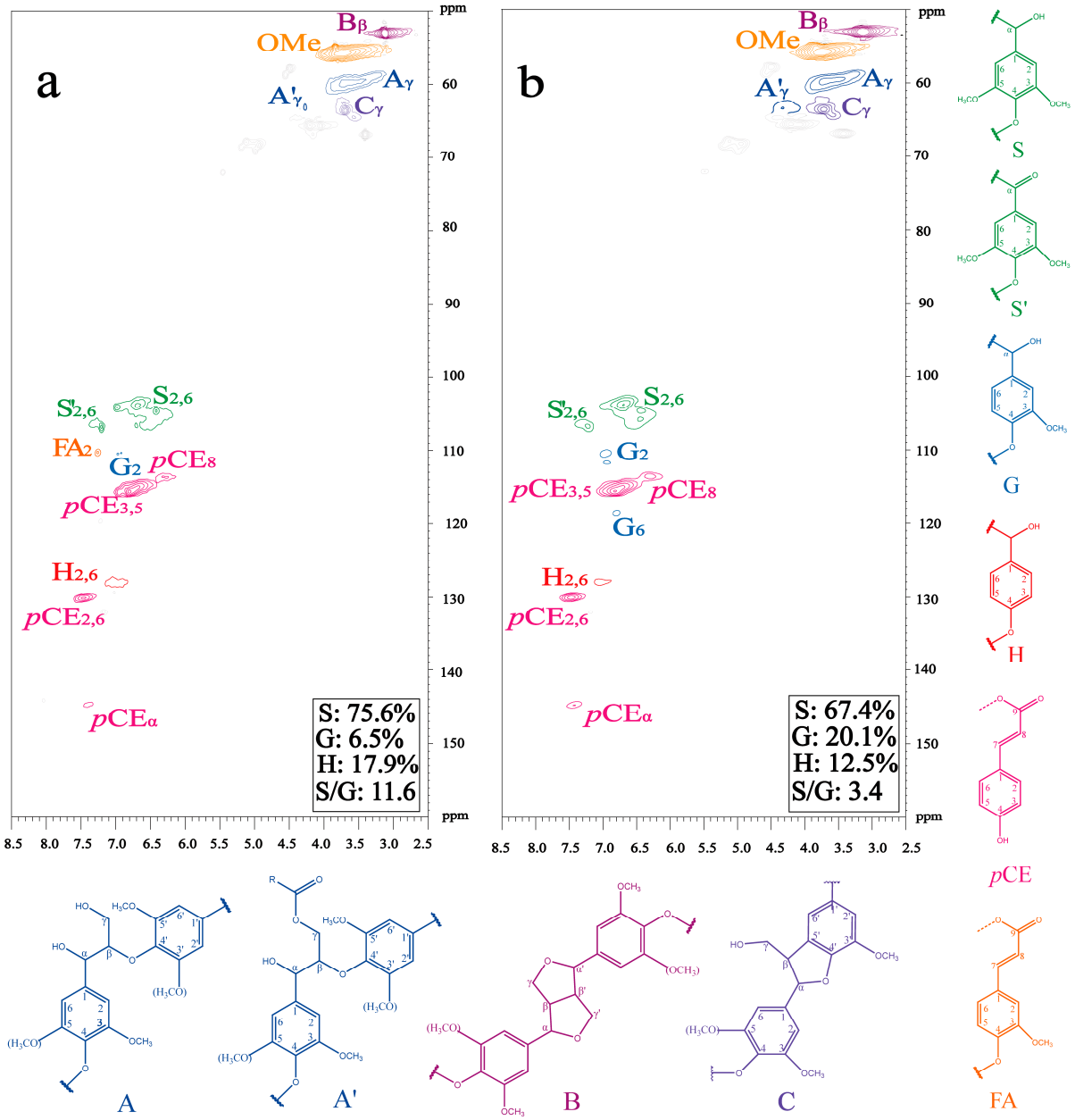


Figure 7. HSQC analysis of DEL obtained via recovered DES: (**a**) the 1st run and (**b**) the 5th run under ChCl:LA (1:3), 140 °C, 2 h, 1 g/10 mL.

3.3. Evaluation of antioxidant activity of DEL

It is generally considered that the lower the lignin concentration (IC_{50}) required for reaching a 50% inhibitory ratio is, the better the antioxidant activity of lignin [20,34,65–67].

The effect of the DEL concentration on its antioxidant activity was investigated, and the results are shown in Figure S3. Compared with other lignin samples reported in previous literature (listed in Table 1), the lower IC_{50} of DEL shows its better antioxidant activity, highlighting that the regenerated lignin obtained from green bamboo after the sequential hydrothermal–DES pretreatment could be well used as natural antioxidant and preservative in industry.

Table 1. Comparison in IC_{50} among lignins from different lignocelluloses using different pretreatment methods.

Lignocellulosic Source	Pretreatment Method	IC_{50} (mg/mL)	Ref.
Bamboo (*bambusa rigida* sp.)	Dimethyl sulfoxide/N-methylimidazole-dissolved lignin	0.06~0.11	[65]
Bamboo (*Phyllostachys pubescen*)	Steam-exploded lignin	0.18~0.50	[66]
Pine wood	Organosolv ethanol lignin	nearly 0.10	[34]
Pennisetum	$FeCl_3$-catalyzed ChCl/glycerol DES pretreatment	0.055~0.115	[20]
Bamboo (*Dendrocalamopsis oldhami*)	Sequential hydrothermal–ChCl/LA DES pretreatment	<0.05	In this work

Dizhbite et al. [68] found that syringyl derivatives (dimethoxy compounds) showed higher antioxidant efficacy than guaiacyl derivatives. It is suggested that the antioxidant activity of DEL from green bamboo after ChCl–LA treatment is higher than that of lignins from different bamboos after different treatments reported in the literature [65,66], mainly owing to a higher S/G ratio in the structure of the former (11.6) (Figure 7a) compared to the others (1.77–2.06 and 2.80–7.60). The slight decrease in DPPH radical scavenging activity for DEL obtained after five runs of ChCl–LA recycling is probably due to the decrease in the S/G ratio from 11.6 to 3.4, as shown in Figure 7. Nevertheless, the recycling of ChCl–LA has no significant influence on the antioxidant activity of DEL.

3.4. Enzymatic Hydrolysis of CR

CR obtained from green bamboo after the sequential hydrothermal–DES pretreatment was employed as feedstock for enzymatic hydrolysis. As shown in Figure S4 (I), the glucose concentration increased with increasing solid loading, whereas the saccharification ratio reached a maximum value of 22.7% at the solid loading of 5%. It is seen from Figure S4 (II) and (III) that the maximum saccharification ratios were 36.2% (increase of 59.7%) with adding Tween-20 at 5 mg/mL, and 37.4% (increase of 64.8%) with adding BSA at 17.5 mg/mL, which probably results from Tween-20 or BSA binding to the residual lignin instead of enzyme and thus reducing the nonproductive adsorption of the enzyme. Moreover, without adding chemical additives, cellulase complexes composed of 60% Cellic CTec3 and 40% PH9018 exhibited a maximum saccharification ratio of 26.0% shown in Figure S4 (IV). From Figure S4 (V–VII), the saccharification ratio was not proportional to cellulase dosage, which is probably due to the limited reaction sites (~1 m^2/g) or the inherent recalcitrance of the substrate. Consequently, considering the cost of the enzymatic saccharification process, the optimum enzymatic conditions are 5% (w/v) of solid loading, Tween-20 at 5 mg/mL, a cellulase dosage of 30 FPU/g_{glucan}, and a Cellic CTec3 percentage of 60% (40% of PH9018), and the corresponding saccharification ratio is 37.2% (marked as dotted line in Figure S4).

Notably, it is observed in Figure 8 that although the enzymatic digestibility of crude green bamboo is low, with a saccharification ratio of 6.5% owing to its inherent recalcitrance, the saccharification ratio of CR (37.2%) is nearly twice as high as that of HTB (20.9%), demonstrating a high efficiency of the integrated hydrothermal–DES pretreatment upon destroying the recalcitrance of green bamboo.

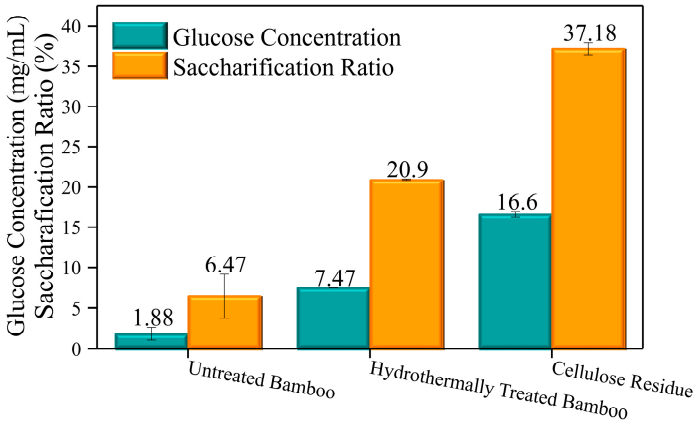


Figure 8. Comparison of enzymatic saccharification among untreated bamboo, hydrothermally treated bamboo, and cellulose residue.

4. Conclusions

The proposed integrated hydrothermal–DES pretreatment is efficient in destroying the recalcitrance of green bamboo into three well-defined components, with hemicellulose and lignin removal of 88.6% and 79.1%, respectively. The comprehensive and value-added utilization of bamboo is achieved by the transformation of hemicellulose, cellulose, and lignin into xylo-oligosaccharides, glucose, and antioxidants. More importantly, ChCl–LA has a superior delignification performance even after five recycling runs, exhibiting the potential to reduce operating cost for industrial consideration.

Supplementary Materials: The following supporting information can be downloaded at: https://www.mdpi.com/article/10.3390/app13042429/s1, Figure S1: The records of experimental temperature to hydrothermal time under different hydrothermal conditions: (**a**) temperature, (**b**) time, and (**c**) solid-to-liquid ratio; Figure S2: Surface morphology of bamboo particles: (**a**) untreated bamboo; hydrothermal pretreatment at (**b**) 160 °C—30 min—3/30 g/mL, (**c**) 170 °C—30 min—3/30 g/mL, (**d**) 180 °C—30 min—3/30 g/mL, (**e**) 190 °C—30 min—-3/30 g/mL, (**f**) 200 °C—30 min—3/30 g/mL, (**g**) 210 °C—30 min—3/30 g/mL, (**h**) 180 °C—20 min—3/30 g/mL, (**i**) 180 °C—35 min—3/30 g/mL, (**j**) 180 °C—40 min—3/30 g/mL, (**k**) 180 °C—45 min—3/30 g/mL, (**l**) 180 °C—50 min—3/30 g/mL, (**m**) 180 °C—35 min—3/24 g/mL, (**n**) 180 °C—35 min—3/36 g/mL, (**o**) 180 °C—35 min—3/42 g/mL, (**p**) 180 °C—35 min—3/48 g/mL, (**q**) 180 °C—35 min—3/60 g/mL; Figure S3: Effect of DEL concentration on inhibitory ratio; Figure S4: Glucose concentration and saccharification ratio during the optimization of enzymatic parameters. (**I**) 30 FPU/g_{glucan} of Cellic CTec3, solid loading of 2–10% (w/v) without chemical additives; (**II**) 30 FPU/g_{glucan} of Cellic CTec3, solid loading of 5% (w/v), a Tween-20 concentration of 5–25 mg/mL; (**III**) 30 FPU/g_{glucan} of Cellic CTec3, solid loading of 5% (w/v), a BSA concentration of 5–25 mg/mL; (**IV**) 30 FPU/g_{glucan} of cellulase complexes with a Cellic CTec3 percentage of 0–100%, solid loading of 5% (w/v) without chemical additives; (**V**) 50 FPU/g_{glucan} of cellulase complexes with a Cellic CTec3 percentage of 0–100%, solid loading of 5% (w/v) without chemical additives; (**VI** 70 FPU/g_{glucan} of cellulase complexes with a Cellic CTec3 percentage of 0–100%, solid loading of 5% (w/v) without chemical additives; (**VII**) 90 FPU/g_{glucan} of cellulase complexes with a Cellic CTec3 percentage of 0–100%, solid loading of 5% (w/v) without chemical additives; Table S1: Characteristic bands of FTIR spectra of bamboo samples; Table S2: Assignments of 13C–1H correlations in the HSQC spectra of lignin from green bamboo.

Author Contributions: Conceptualization, L.G. and K.S.; validation, J.S., Y.X., Q.C. and S.Y.; formal analysis, L.C., J.S., R.Y. and Y.X.; investigation, L.C. and R.Y.; writing—original draft preparation, L.C.; writing—review and editing, L.G., K.S. and L.C.; visualization, L.C., Q.C. and S.Y.; supervision, L.G.; project administration, L.G. All authors have read and agreed to the published version of the manuscript.

Funding: This research was funded by the Guiding Project of Science and Technology Plan of Fujian Province, China, grant number 2020N0011.

Institutional Review Board Statement: Not applicable.

Informed Consent Statement: Not applicable.

Data Availability Statement: The data presented in this study are available on request from the corresponding author.

Acknowledgments: The authors greatly appreciate the analysis support provided by Instrumental Analysis Center of Huaqiao University of China and Institute of Urban Environment, Chinese Academy of Sciences. The authors also thank Kenan Li, Yun Zhan, Ying Cui, and Guobao Sima for their invaluable input.

Conflicts of Interest: The authors declare no conflict of interest.

References

1. Niu, D.; Wu, G.; Ji, Z.; Wang, D.; Li, Y.; Gao, T. Evaluation of Provincial Carbon Neutrality Capacity of China Based on Combined Weight and Improved TOPSIS Model. *Sustainability* **2021**, *13*, 2777. [CrossRef]
2. Pilpola, S.; Arabzadeh, V.; Mikkola, J.; Lund, P.D. Analyzing National and Local Pathways to Carbon-Neutrality from Technology, Emissions, and Resilience Perspectives—Case of Finland. *Energies* **2019**, *12*, 949. [CrossRef]
3. Wang, Y.; Guo, C.; Zhuang, S.; Chen, X.; Jia, L.; Chen, Z.; Xia, Z.; Wu, Z. Major contribution to carbon neutrality by China's geosciences and geological technologies. *China Geol.* **2021**, *4*, 329–352. [CrossRef]
4. Zhou, B.; Fu, M.; Xie, J.; Yang, X.; Li, Z. Ecological functions of bamboo forest: Research and Application. *J. For. Res.* **2005**, *16*, 143–147. [CrossRef]
5. McCallum, C.S.; Wang, W.; Doran, W.J.; Forsythe, W.G.; Garrett, M.D.; Hardacre, C.; Leahy, J.J.; Morgan, K.; Shin, D.-S.; Sheldrake, G.N. Life cycle thinking case study for catalytic wet air oxidation of lignin in bamboo biomass for vanillin production. *Green Chem.* **2021**, *23*, 1847–1860. [CrossRef]
6. Li, Z.; Chen, C.; Mi, R.; Gan, W.; Dai, J.; Jiao, M.; Xie, H.; Yao, Y.; Xiao, S.; Hu, L. A Strong, Tough, and Scalable Structural Material from Fast-Growing Bamboo. *Adv. Mater.* **2020**, *32*, 1906308. [CrossRef] [PubMed]
7. Buziquia, S.T.; Lopes, P.V.F.; Almeida, A.K.; de Almeida, I.K. Impacts of bamboo spreading: A review. *Biodivers. Conserv.* **2019**, *28*, 3695–3711. [CrossRef]
8. Kumari, D.; Singh, R. Pretreatment of lignocellulosic wastes for biofuel production: A critical review. *Renew. Sust. Energy Rev.* **2018**, *90*, 877–891. [CrossRef]
9. Kumar, A.K.; Sharma, S. Recent updates on different methods of pretreatment of lignocellulosic feedstocks: A review. *Bioresour. Bioprocess.* **2017**, *4*, 7. [CrossRef] [PubMed]
10. Cheah, W.Y.; Sankaran, R.; Show, P.L.; Tg. Ibrahim, T.N.B.; Chew, K.W.; Culaba, A.; Chang, J.-S. Pretreatment methods for lignocellulosic biofuels production: Current advances, challenges and future prospects. *Biofuel Res. J.* **2020**, *7*, 1115–1127. [CrossRef]
11. Hassan, S.S.; Williams, G.A.; Jaiswal, A.K. Emerging technologies for the pretreatment of lignocellulosic biomass. *Bioresour. Technol.* **2018**, *262*, 310–318. [CrossRef] [PubMed]
12. Peterson, A.A.; Vogel, F.; Lachance, R.P.; Fröling, M.; Antal, J.M.J.; Tester, J.W. Thermochemical biofuel production in hydrothermal media: A review of sub- and supercritical water technologies. *Energy Environ. Sci.* **2008**, *1*, 32–65. [CrossRef]
13. Santibanez, L.; Henriquez, C.; Corro-Tejeda, R.; Bernal, S.; Armijo, B.; Salazar, O. Xylooligosaccharides from lignocellulosic biomass: A comprehensive review. *Carbohydr. Polym.* **2021**, *251*, 117118. [CrossRef] [PubMed]
14. Questell-Santiago, Y.M.; Galkin, M.V.; Barta, K.; Luterbacher, J.S. Stabilization strategies in biomass depolymerization using chemical functionalization. *Nat. Rev. Chem.* **2020**, *4*, 311–330. [CrossRef]
15. Bobleter, O. Hydrothermal degradation of polymers derived from plants. *Prog. Polym. Sci.* **1994**, *19*, 797–841. [CrossRef]
16. Zheng, B.A.; Zhu, Y.K.; Zheng, S.H.; Mo, Y.; Sun, S.L.; Ren, J.L.; Li, Y.H.; Wu, A.M.; Li, H.L. Upgrade the torrefaction process of bamboo based on autohydrolysis pretreatment. *Ind. Crops Prod.* **2021**, *166*, 113470. [CrossRef]
17. Xiao, X.; Bian, J.; Peng, X.P.; Xu, H.; Xiao, B.; Sun, R.C. Autohydrolysis of bamboo (Dendrocalamus giganteus Munro) culm for the production of xylo-oligosaccharides. *Bioresour. Technol.* **2013**, *138*, 63–70. [CrossRef]
18. Huang, C.; Fang, G.; Zhou, Y.; Du, X.; Yu, L.; Meng, X.; Li, M.; Yoo, C.G.; Chen, B.; Zhai, S.; et al. Increasing the Carbohydrate Output of Bamboo Using a Combinatorial Pretreatment. *ACS Sustain. Chem. Eng.* **2020**, *8*, 7380–7393. [CrossRef]
19. Tsubota, T.; Ishimoto, K.; Kumagai, S.; Kamimura, S.; Ohno, T. Cascade use of bamboo as raw material for several high value products: Production of xylo-oligosaccharide and activated carbon for EDLC electrode from bamboo. *J. Porous Mater.* **2018**, *25*, 1541–1549. [CrossRef]
20. Wang, Z.; Hong, S.; Wen, J.; Ma, C.; Tang, L.; Jiang, H.; Chen, J.; Li, S.; Shen, X.; Yuan, T. Lewis Acid-Facilitated Deep Eutectic Solvent (DES) Pretreatment for Producing High-Purity and Antioxidative Lignin. *ACS Sustain. Chem. Eng.* **2020**, *8*, 1050–1057. [CrossRef]
21. Amesho, K.T.T.; Lin, Y.-C.; Mohan, S.V.; Halder, S.; Ponnusamy, V.K.; Jhang, S.-R. Deep eutectic solvents in the transformation of biomass into biofuels and fine chemicals: A review. *Environ. Chem. Lett.* **2022**, 1–48. [CrossRef]

22. Lee, C.B.T.L.; Wu, T.Y.; Cheng, C.K.; Siow, L.F.; Chew, I.M.L. Nonsevere furfural production using ultrasonicated oil palm fronds and aqueous choline chloride-oxalic acid. *Ind. Crops Prod.* **2021**, *166*, 113397. [CrossRef]
23. Smith, E.L.; Abbott, A.P.; Ryder, K.S. Deep eutectic solvents (DESs) and their applications. *Chem. Rev.* **2014**, *114*, 11060–11082. [CrossRef] [PubMed]
24. Sharma, V.; Tsai, M.L.; Chen, C.W.; Sun, P.P.; Patel, A.K.; Singhania, R.R.; Nargotra, P.; Dong, C.D. Deep eutectic solvents as promising pretreatment agents for sustainable lignocellulosic biorefineries: A review. *Bioresour. Technol.* **2022**, *360*, 127631. [CrossRef]
25. Fernandes, C.; Melro, E.; Magalhaes, S.; Alves, L.; Craveiro, R.; Filipe, A.; Valente, A.J.M.; Martins, G.; Antunes, F.E.; Romano, A.; et al. New deep eutectic solvent assisted extraction of highly pure lignin from maritime pine sawdust (*Pinus pinaster* Ait.). *Int. J. Biol. Macromol.* **2021**, *177*, 294–305. [CrossRef]
26. Komesu, A.; Martins Martinez, P.F.; Lunelli, B.H.; Oliveira, J.; Wolf Maciel, M.R.; Maciel Filho, R. Study of Lactic Acid Thermal Behavior Using Thermoanalytical Techniques. *J. Chem.* **2017**, *2017*, 1–7. [CrossRef]
27. Tan, Y.T.; Ngoh, G.C.; Chua, A.S.M. Effect of functional groups in acid constituent of deep eutectic solvent for extraction of reactive lignin. *Bioresour. Technol.* **2019**, *281*, 359–366. [CrossRef]
28. Wang, R.; Wang, K.; Zhou, M.; Xu, J.; Jiang, J. Efficient fractionation of moso bamboo by synergistic hydrothermal-deep eutectic solvents pretreatment. *Bioresour. Technol.* **2021**, *328*, 124873. [CrossRef]
29. Lin, W.Q.; Xing, S.; Jin, Y.C.; Lu, X.M.; Huang, C.X.; Yong, Q. Insight into understanding the performance of deep eutectic solvent pretreatment on improving enzymatic digestibility of bamboo residues. *Bioresour. Technol.* **2020**, *306*, 123163. [CrossRef]
30. Liu, Q.; Yuan, T.; Fu, Q.; Bai, Y.; Peng, F.; Yao, C. Choline chloride-lactic acid deep eutectic solvent for delignification and nanocellulose production of moso bamboo. *Cellulose* **2019**, *26*, 9447–9462. [CrossRef]
31. Datta, R. Acidogenic Fermentation of Lignocellulose-Acid Yield and Conversion of Components. *Biotechnol. Bioeng.* **1981**, *23*, 2167–2170. [CrossRef]
32. Cheng, F.; Zhao, X.; Hu, Y. Lignocellulosic biomass delignification using aqueous alcohol solutions with the catalysis of acidic ionic liquids: A comparison study of solvents. *Bioresour. Technol.* **2018**, *249*, 969–975. [CrossRef]
33. Guo, S.; Dong, X.; Zhu, C.; Han, Y.; Ma, F.; Wu, T. Pyrolysis behaviors and thermodynamics properties of hydrochar from bamboo (*Phyllostachys heterocycla* cv. pubescens) shoot shell. *Bioresour. Technol.* **2017**, *233*, 92–98. [CrossRef]
34. Liu, D.; Li, Y.; Qian, Y.; Xiao, Y.; Du, S.; Qiu, X. Synergistic Antioxidant Performance of Lignin and Quercetin Mixtures. *ACS Sustain. Chem. Eng.* **2017**, *5*, 8424–8428. [CrossRef]
35. Sluiter, A.; Hames, B.; Ruiz, R.; Scarlata, C.; Sluiter, J.; Templeton, D.; Crocker, D. Determination of Structural Carbohydrates and Lignin in Biomass, Laboratory Analytical Procedure (LAP): Technical Report NREL/TP-510-42618. *Natl. Renew. Energy Lab. (NREL)* **2012**, *1617*, 1–15.
36. Segal, L.; Creely, J.J.; Martin, A.E.; Conrad, C.M. An empirical method for estimating the degree of crystallinity of native cellulose using the X-ray diffractometer. *Text. Res. J.* **1959**, *29*, 786–794. [CrossRef]
37. Cao, X.; Peng, X.; Sun, S.; Zhong, L.; Sun, R. Hydrothermal conversion of bamboo: Identification and distribution of the components in solid residue, water-soluble and acetone-soluble fractions. *J. Agric. Food. Chem.* **2014**, *62*, 12360–12365. [CrossRef] [PubMed]
38. Donohoe, B.S.; Decker, S.R.; Tucker, M.P.; Himmel, M.E.; Vinzant, T.B. Visualizing lignin coalescence and migration through maize cell walls following thermochemical pretreatment. *Biotechnol. Bioeng.* **2008**, *101*, 913–925. [CrossRef] [PubMed]
39. Yue, P.P.; Hu, Y.J.; Fu, G.Q.; Sun, C.X.; Li, M.F.; Peng, F.; Sun, R.C. Structural Differences between the Lignin-Carbohydrate Complexes (LCCs) from 2- and 24-Month-Old Bamboo (*Neosinocalamus affinis*). *Int. J. Mol. Sci.* **2017**, *19*, 1. [CrossRef] [PubMed]
40. Wang, F.; Li, S.; Sun, Y.; Han, H.; Zhang, B.; Hu, B.; Gao, Y.; Hu, X. Ionic liquids as efficient pretreatment solvents for lignocellulosic biomass. *RSC Adv.* **2017**, *7*, 47990–47998. [CrossRef]
41. Sirviö, J.A.; Visanko, M. Anionic wood nanofibers produced from unbleached mechanical pulp by highly efficient chemical modification. *J. Mater. Chem. A* **2017**, *5*, 21828–21835. [CrossRef]
42. An, Y.; Li, N.; Wu, H.; Lou, W.; Zong, M. Changes in the Structure and the Thermal Properties of Kraft Lignin during Its Dissolution in Cholinium Ionic Liquids. *ACS Sustain. Chem. Eng.* **2015**, *3*, 2951–2958. [CrossRef]
43. Yang, H.; Jin, Y.; Shi, Z.; Wang, D.; Zhao, P.; Yang, J. Effect of hydrothermal pretreated bamboo lignin on cellulose saccharification for bioethanol production. *Ind. Crops Prod.* **2020**, *156*, 112865. [CrossRef]
44. Xu, G.; Wang, L.; Liu, J.; Wu, J. FTIR and XPS analysis of the changes in bamboo chemical structure decayed by white-rot and brown-rot fungi. *Appl. Surf. Sci.* **2013**, *280*, 799–805. [CrossRef]
45. Wu, K.; Ying, W.; Shi, Z.; Yang, H.; Zheng, Z.; Zhang, J.; Yang, J. Fenton Reaction-Oxidized Bamboo Lignin Surface and Structural Modification to Reduce Nonproductive Cellulase Binding and Improve Enzyme Digestion of Cellulose. *ACS Sustain. Chem. Eng.* **2018**, *6*, 3853–3861. [CrossRef]
46. Luo, X.; Liu, J.; Wang, H.; Huang, L.; Chen, L. Comparison of hot-water extraction and steam treatment for production of high purity-grade dissolving pulp from green bamboo. *Cellulose* **2014**, *21*, 1445–1457. [CrossRef]
47. Wen, J.L.; Sun, S.L.; Xue, B.L.; Sun, R.C. Quantitative structures and thermal properties of birch lignins after ionic liquid pretreatment. *J. Agric. Food. Chem.* **2013**, *61*, 635–645. [CrossRef]
48. Liu, B.; Li, T.; Wang, W.; Sagis, L.M.C.; Yuan, Q.; Lei, X.; Cohen Stuart, M.A.; Li, D.; Bao, C.; Bai, J.; et al. Corncob cellulose nanosphere as an eco-friendly detergent. *Nat. Sustain.* **2020**, *3*, 448–458. [CrossRef]

49. Cvjetko Bubalo, M.; Curko, N.; Tomasevic, M.; Kovacevic Ganic, K.; Radojcic Redovnikovic, I. Green extraction of grape skin phenolics by using deep eutectic solvents. *Food Chem.* **2016**, *200*, 159–166. [CrossRef]
50. Kumar, A.K.; Parikh, B.S.; Pravakar, M. Natural deep eutectic solvent mediated pretreatment ofrice straw: Bioanalytical characterization of lignin extract and enzymatic hydrolysis of pretreated biomass residue. *Environ. Sci. Pollut. Res.* **2016**, *23*, 9265–9275. [CrossRef]
51. Hu, F.; Jung, S.; Ragauskas, A. Pseudo-lignin formation and its impact on enzymatic hydrolysis. *Bioresour. Technol.* **2012**, *117*, 7–12. [CrossRef] [PubMed]
52. Sannigrahi, P.; Kim, D.H.; Jung, S.; Ragauskas, A. Pseudo-lignin and pretreatment chemistry. *Energy Environ. Sci.* **2011**, *4*, 1306–1310. [CrossRef]
53. Chang, L.; Sun, Y.; Gan, L. Insights into cellulose deconstruction and pseudo-lignin formation during deep eutectic solvent treatment. *Cellulose* **2022**, *30*, 141–152. [CrossRef]
54. Sethi, J.; Farooq, M.; Sain, S.; Sain, M.; Sirviö, J.A.; Illikainen, M.; Oksman, K. Water resistant nanopapers prepared by lactic acid modified cellulose nanofibers. *Cellulose* **2017**, *25*, 259–268. [CrossRef]
55. Shen, X.; Wen, J.; Mei, Q.; Chen, X.; Sun, D.; Yuan, T.; Sun, R. Facile fractionation of lignocelluloses by biomass-derived deep eutectic solvent (DES) pretreatment for cellulose enzymatic hydrolysis and lignin valorization. *Green Chem.* **2019**, *21*, 275–283. [CrossRef]
56. Ci, Y.-H.; Yu, F.; Zhou, C.-X.; Mo, H.-E.; Li, Z.-Y.; Ma, Y.-Q.; Zang, L.-H. New ternary deep eutectic solvents for effective wheat straw deconstruction into its high-value utilization under near-neutral conditions. *Green Chem.* **2020**, *22*, 8713–8720. [CrossRef]
57. Kim, K.H.; Dutta, T.; Sun, J.; Simmons, B.; Singh, S. Biomass Pretreatment using Deep Eutectic Solvent from Lignin derived Phenols. *Green Chem.* **2018**, *20*, 809–815. [CrossRef]
58. Wang, W.; Tan, X.; Yu, Q.; Wang, Q.; Qi, W.; Zhuang, X.; Wang, Z.; Yuan, Z. Effect of stepwise lignin removal on the enzymatic hydrolysis and cellulase adsorption. *Ind. Crops Prod.* **2018**, *122*, 16–22. [CrossRef]
59. Wen, J.; Xue, B.; Xu, F.; Sun, R. Unveiling the Structural Heterogeneity of Bamboo Lignin by In Situ HSQC NMR Technique. *Bioenerg. Res.* **2012**, *5*, 886–903. [CrossRef]
60. Wen, J.; Sun, S.; Xue, B.; Sun, R. Quantitative structural characterization of the lignins from the stem and pith of bamboo (*Phyllostachys pubescens*). *Holzforschung* **2013**, *67*, 613–627. [CrossRef]
61. Cao, Q.; Wu, Q.; Dai, L.; Shen, X.; Si, C. A well-defined lignin-based filler for tuning the mechanical properties of polymethyl methacrylate. *Green Chem.* **2021**, *23*, 2329–2335. [CrossRef]
62. Hong, S.; Shen, X.; Pang, B.; Xue, Z.; Cao, X.; Wen, J.; Sun, Z.; Lam, S.S.; Yuan, T.; Sun, R. In-depth interpretation of the structural changes of lignin and formation of diketones during acidic deep eutectic solvent pretreatment. *Green Chem.* **2020**, *22*, 1851–1858. [CrossRef]
63. Rencoret, J.; Marques, G.; Gutiérrez, A.; Nieto, L.; Jiménez-Barbero, J.; Martínez, Á.T.; del Río, J.C. Isolation and structural characterization of the milled-wood lignin from Paulownia fortunei wood. *Ind. Crops Prod.* **2009**, *30*, 137–143. [CrossRef]
64. Chen, T.Y.; Wen, J.L.; Wang, B.; Wang, H.M.; Liu, C.F.; Sun, R.C. Assessment of integrated process based on autohydrolysis and robust delignification process for enzymatic saccharification of bamboo. *Bioresour. Technol.* **2017**, *244*, 717–725. [CrossRef]
65. Wen, J.; Xue, B.; Xu, F.; Sun, R.; Pinkert, A. Unmasking the structural features and property of lignin from bamboo. *Ind. Crops Prod.* **2013**, *42*, 332–343. [CrossRef]
66. Sun, S.; Wen, J.; Ma, M.; Sun, R.; Jones, G.L. Structural features and antioxidant activities of degraded lignins from steam exploded bamboo stem. *Ind. Crops Prod.* **2014**, *56*, 128–136. [CrossRef]
67. Pan, X.; Kadla, J.F.; Ehara, K.; Gilkes, N.; Saddler, J.N. Organosolv Ethanol Lignin from Hybrid Poplar as a Radical Scavenger: Relationship between Lignin Structure, Extraction Conditions, and Antioxidant Activity. *J. Agric. Food Chem.* **2006**, *54*, 5806–5813. [CrossRef]
68. Dizhbite, T.; Telysheva, G.; Jurkjane, V.; Viesturs, U. Characterization of the radical scavenging activity of lignins–natural antioxidants. *Bioresour. Technol.* **2004**, *95*, 309–317. [CrossRef]

Disclaimer/Publisher's Note: The statements, opinions and data contained in all publications are solely those of the individual author(s) and contributor(s) and not of MDPI and/or the editor(s). MDPI and/or the editor(s) disclaim responsibility for any injury to people or property resulting from any ideas, methods, instructions or products referred to in the content.